LUNAR HYPERSPECTRAL IMAGE DESTRIPING METHOD USING LOW-RANK MATRIX RECOVERY AND GUIDED PROFILE

Shuheng Zhao¹, Qiangqiang Yuan², Member, IEEE, Jie Li², Member, IEEE, Huanfeng Shen³, Senior Member, IEEE, Liangpei Zhang¹, Fellow, IEEE

¹ State Key Laboratory of Information Engineering, Survey Mapping and Remote Sensing, Wuhan University, P. R. China.

² School of Geodesy and Geomatics, Wuhan University, P.R. China. ³ School of Resource and Environmental Science, Wuhan University, P. R. China.

ABSTRACT

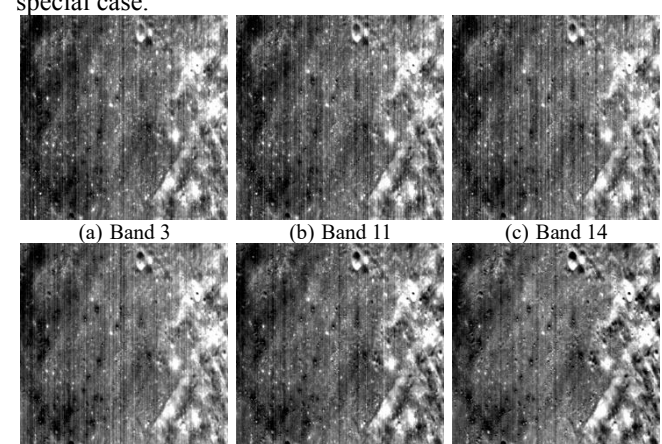
The lunar hyperspectral remote sensing is one of the most important means to understand the physical properties and chemical constituents of lunar surface materials. Moon Mineral Mapper (M³) is currently the only hyperspectral image (HSI) data of Moon. However, due to the limitations of sensor manufacture and the impact of complex extraterrestrial environment, there are serious stripes on the M³ images, which do harm to subsequent identifications and analysis. In this paper, an effective destriping algorithm for lunar HSIs based on the intrinsic characteristics of the stripes on M³ is proposed. Experimental results demonstrate that our method shows an improvement in terms of visual perception and spectral fidelity.

Index Terms— destriping, hyperspectral image, Moon Mineral Mapper, low-rank matrix recovery, mean cross-track profile

1. INTRODUCTION

Moon is the first station of human deep space exploration and also one of the most essential targets [1]. Lunar detection is of great scientific significance for understanding the formation and evolution of the Earth-Moon system and even the entire solar system, and for the development and utilization of the lunar resources [2]. Because of the huge technical risks and financial expenses of manned landing, the remote sensing is still the main method of lunar exploration. Hyperspectral remote sensing technique is an important means to simultaneously obtain the lunar surface material distribution and spectral features therein. But hyperspectral imaging sensors usually suffer from unpredictable environments and instrumental factors. Moon Mineral Mapper (M³) [3], as the sole hyperspectral imaging equipment, is inevitably affected by stripe noises. This kind of unique and dense stripes are spread over every band of M³ with different spatial position and intensity. Meanwhile, they are fairly close to the intrinsic texture of the image itself, as

if embed in the image. This type of stripe is called embedded stripe in this paper. The presence of embedded stripe will interfere with the analysis through the spectral parameter maps and reduce the accuracy of subsequent applications. Therefore, a stripe removal algorithm is needed for this special case.



(d) Band 20 (e) Band 39 (f) Band 59 Fig. 1. Various positions and intensities of embedded stripes on M³

So far, the existing hyperspectral image (HSI) destriping methods are mainly divided into two categories. The first type is to treat each band of the HSI as a single grayscale image, and remove the stripes band by band [4-6]. Although they can effectively remove stripe noises, the continuous spectral signatures are not fully adopted, causing the low spectral fidelity. They are not conducive to following processing. The second type is to restore the whole HSI as a 2-d matrix or 3-d tensor by combing both spatial and spectral information [7-10]. They perform well under the condition of mixed noises and own high spectral fidelity. Nevertheless, for dense and wide stripes, they cannot achieve an ideal effect.

Based on the advantages of two types of pioneer works, we propose a destriping algorithm for M³ datasets which only contain dense embedded stripes and do not contaminated by random noises. The statistical characteristics along the stripe direction of each band are explored to obtain the target

distribution, and then they are integrated into the low-rank matrix recovery to restore spatial and spectral information of the entire HSI. Experimental results show that the proposed algorithm is effective and keeps a high spectral fidelity.

2. METHODOLOGY

1) Regularized Hyperspectral Destriping Model

Assuming that there is a clean HSI, and the stripe noises are regarded as the additive noise, then the stripe contaminated model can be written as:

$$Y = X + S \tag{1}$$

where **Y** is the observed HSI, **X** is the clean HSI that is needed to be obtained, and **S** stands for the embedded stripe noise. Then the destriping model for HSI can be represented as the following regularization-based problem:

$$\hat{\mathbf{X}} = \underset{\mathbf{X},\mathbf{S}}{\operatorname{arg\,min}} R(\mathbf{X}) + \lambda \|\mathbf{Y} - \mathbf{X} - \mathbf{S}\|_{F}^{2}$$
 (2)

In (2), $R(\mathbf{X})$ is the regularization term, offering a prior of the original clean HSI. While $\|\mathbf{Y} - \mathbf{X} - \mathbf{S}\|_F^2$ is the data fidelity item, denoting the fidelity between the clean image and the striped observed image. And λ stands for the regularization parameter, which balances the contributions of the regularization item and imaged fidelity item.

In this work, two constraints are enforced on the clean HSI. One is the guided profile which has the same tendency but smoother compared with the mean profile of the observed HSI. the other one is the low-rank prior. Moreover, the guided profile can be used as the data fidelity terms. The HSI without stripes is low-rank, consequently this constraint can capture the natural spatial structure and maintain the spectral signatures. By explicitly incorporating two priors with the adequate regularization parameters, the final model can be formulated as the following optimization problem:

$$\hat{\mathbf{X}} = \underset{\mathbf{X}}{\arg\min} \| \mathbf{\mathcal{X}} \|_* + \lambda \sum_{i=1}^B \| \hat{\mathbf{g}}(\mathbf{Y}_i) - \mathbf{X}_i \mathbf{f} \|_F^2$$
 (3)

where \mathcal{X} denotes the Casorati matrix of the observed HSI, \mathbf{X}_i and \mathbf{Y}_i stand for the i th band of the clean and striped HSIs respectively. $\hat{\mathbf{g}}(\mathbf{Y})$ is the guided profile of observed HSI \mathbf{Y} , and it will be introduced later. $\mathbf{f} \in R^{n \times 1}$ is a column vector with elements equivalent to 1/n.

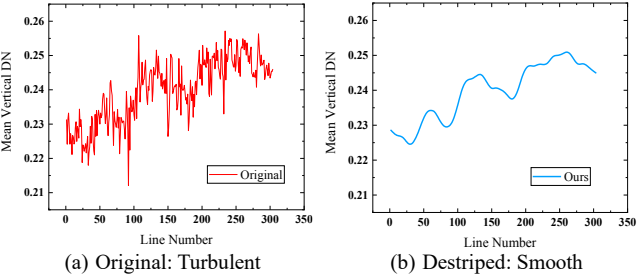


Fig. 2. Illustration of guided profile

2) Guided Profile

The solution of the guided profile under the dense stripe case can be considered as the Hodrick-Prescott filter:

$$\hat{\mathbf{g}}_{i} = \arg\min_{\sigma} \left\| \hat{\mathbf{g}} \left(\mathbf{Y}_{i} \right) - \mathbf{X}_{i} \mathbf{f} \right\|_{F}^{2} + \lambda_{2} \left\| \mathbf{D} \mathbf{g}_{i} \right\|_{F}^{2}$$
(4)

 λ_2 controls the smoothness of the desired profile and **D** is a gaussian blur matrix of the blur kernel $\begin{bmatrix} 1 - 2 \ 1 \end{bmatrix}^T$. (4) can be easily solved by least-squares minimization.

3) Optimization

After getting $\hat{\mathbf{g}}(\mathbf{Y})$, it can be brought into (2) which can be effectively solved by alternating direction multiplier (ADMM) method. One auxiliary variable $\mathbf{H} = \mathcal{X}$ is introduced to convert this problem into two simple subproblems.

The subproblem of **H** is:

$$\mathbf{H} = \arg\min_{\mathbf{H}} \|\mathbf{H}\|_{*} + \frac{\mu}{2} \|\mathbf{H} - \mathbf{X}_{i} + \mathbf{J}_{1}/\mu\|_{F}^{2}$$
 (5)

and it can be easily solved using the singular values thresholding algorithm.

The subproblem of X_i is:

$$\mathbf{X}_{i} = \arg\min_{\mathbf{H}} \left\| \hat{\mathbf{g}} \left(\mathbf{Y}_{i} \right) - \mathbf{X}_{i} \mathbf{f} \right\|_{F}^{2} + \frac{\mu}{2} \left\| \mathbf{H} - \mathbf{X}_{i} + \mathbf{J}_{1} / \mu \right\|_{F}^{2}$$
 (6)

which can be calculated via the least-squares minimization:

$$\mathbf{X}_{i}^{k+1} = \frac{1}{2\lambda} \left(2\lambda \hat{\mathbf{g}} \mathbf{f}^{T} + \mu \mathbf{H}^{k} + \mathbf{J} \right) / \left(\mathbf{f} \mathbf{f}^{T} + \frac{\mu}{2\lambda} \mathbf{I} \right)$$
(7)

Finally, the Lagrangian multiplier and penalization parameters are updated as follows:

$$\mathbf{J}^{k+1} = \mathbf{J}^k + \mu (\mathbf{H}^k - \mathbf{X}^k)$$
 (8)

$$\mu^{k+1} = \rho \times \mu^k \tag{9}$$

3. EXPERIMENTS AND RESULTS

Because the features contained in lunar images are totally different from those in terrestrial images, and the dense embedded stripes are difficult to simulate, only real experiments are conducted in this paper. The 300×300 pixels interests of area of the landing site of Chang'E 4 is selected. After excluding two bands without valid information, the final $300\times300\times83$ image ranging from $620\sim2980$ nm is employed in the experiments.

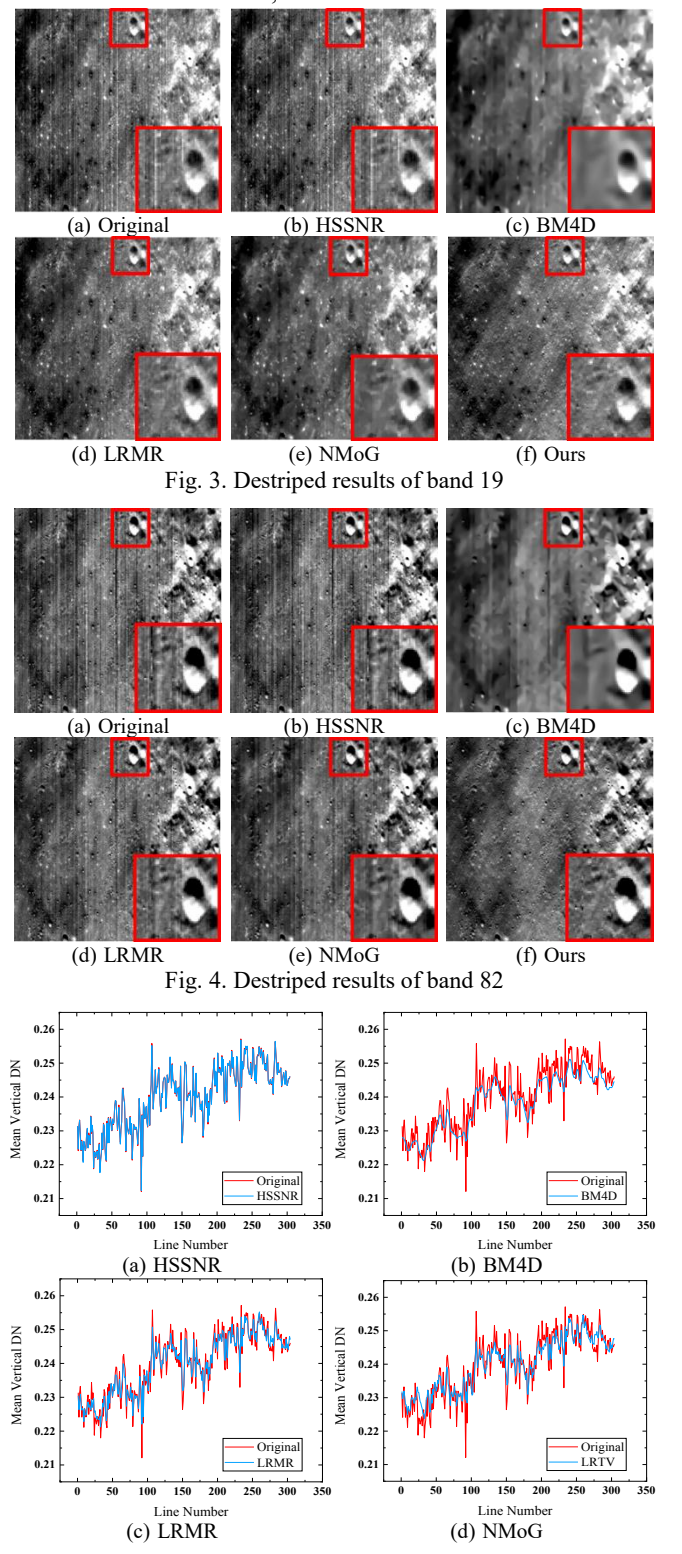
For quantitatively assess and compare the performance of our method and others, two nonreference indicators are chosen. The first one is the mean inverse coefficient of variations (MICV), which evaluates the level of residual stripe noises. The other one is the mean relative deviation (MRD), which calculates the noise-free region's change and rates the capability of keeping the original healthy information. They are defined as follows:

MICV=
$$\frac{1}{B} \times \sum_{i=1}^{B} \frac{R_{m_i}}{R_{s_i}}$$
 (10)

$$MRD = \frac{1}{MNB} \times \sum_{i=1}^{B} \sum_{j=1}^{M} \sum_{k=1}^{N} \frac{|\hat{x} - y|}{y} \times 100\%$$
 (11)

where R_{m-i} and R_{s-i} stand for the mean and standard devia-

tion of the *i* th band, and \hat{x} and y are the pixel values in the estimated and original images respectively. The higher MICV is and the lower MRD is, the better the result is.



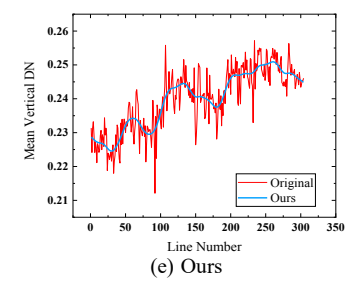


Fig. 6. The mean vertical profile after destriping

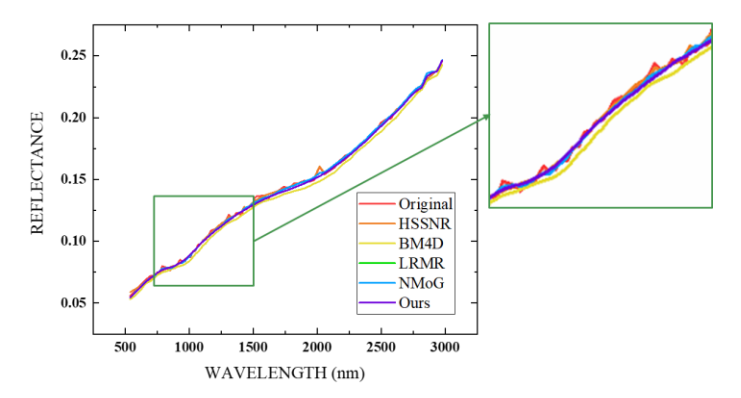


Fig. 6. Intercomparison of destriped spectral signatures

TABLE I QUANTITATIVE INDICATORS

Index	Original	HSSNR	BM4D	LRMR	NMoG	Ours
MICV	1.258	1.987	2.763	29.547	28.862	31.098
MRD	-	12.875	11.735	2.116	3.240	0.717

Through visual effects in Fig. 3 and Fig. 4 and the quantitative indicators in Table I, it can be seen that our method overperforms compared with other algorithms in numerical indices, and totally removes the dense embedded stripes which others cannot. As shown in Fig. 5, our method can efficiently smooth the turbulence of the spectral signals, bringing convenience to following processing and analysis. Moreover, Fig. 6 depicts that the proposed model has the same high spectral fidelity with other state-of-the-art methods while smooth the spiky impact on the spectral signatures.

4. CONCLUSION

In this paper, a destriping method which targets at the embedding stripe noises on M³ imagery has been proposed. From the perspective of the statistical feature along the stripe direction of the image, a guided profile is utilized to constraint the values of embedding stripes. Meanwhile the guided profile is incorporated into the low-rank matrix recovery, which restores the spatial structure and the spectral information of the whole HSI. The real experiments conducted on M³ images show illustrate that our method overperforms other algorithms. It can totally remove the dense and embedding stripe noises while keeping a good spectral fidelity.

Based on the great results of the proposed method, we plan to employ the destriped M³ images to check the recovery of the spectral parameter maps, and further quantitatively evaluate the performance of our algorithm throaty applications and analysis such as the mineral extraction.

5. REFERENCES

- [1] Z. Ouyang, "SCIENTIFIC OBJECTIVES OF CHINESE LUNAR EXPLORATION PROJECT AND DEVELOPMENT STRATEGY," *ADVANCE IN EARTH SCIENCES*, vol. Issue, no. 3, 2004.
- [2] B. L. Kaichang Di, Zhaoqin Liu, Yongliao Zhou, "Review and prospect of lunar mapping using remote sensing data. Journal of Remote Sensing," *Journal of Remote Sensing*, vol. 20, p. 13, 2016.
- [3] R. O. Green et al., "The Moon Mineralogy Mapper Imaging Spectrometer: Instrument Description, Calibration, and On-Orbit Validation of the Spectral, Radiometric, Spatial and Uniformity Characteristics (Invited)," presented at the AGU Fall Meeting Abstracts, December 01, 2009, 2009.
- [4] Jinsong Chen, Yun Shao, Huadong Guo, Weiming Wang, and Boqin Zhu, "Destriping CMODIS data by power filtering," IEEE Transactions on Geoscience & Remote Sensing, vol. 41, no. 9, pp. 2119-2124.
- [5] R. Pande-Chhetri and A. Abd-Elrahman, "De-striping hyperspectral imagery using wavelet transform and adaptive frequency domain filtering," ISPRS Journal of Photogrammetry and Remote Sensing, vol. 66, pp. 620-636, September 01, 2011 2011.
- [6] X. Liu, H. Shen, Q. Yuan, X. Lu, and C. Zhou, "A Universal Destriping Framework Combining 1-D and 2-D Variational Optimization Methods," IEEE Transactions on Geoscience and Remote Sensing, vol. 56, pp. 808-822, February 01, 2018 2018.
- [7] H. Othman and S.-E. Qian, "Noise Reduction of Hyperspectral Imagery Using Hybrid Spatial-Spectral Derivative-Domain Wavelet Shrinkage," IEEE Transactions on Geoscience and Remote Sensing, vol. 44, pp. 397-408, February 01, 2006 2006.
- [8] M. Maggioni, V. Katkovnik, K. Egiazarian, and A. Foi, "Nonlocal Transform-Domain Filter for Volumetric Data Denoising and Reconstruction," IEEE Transactions on Image Processing, vol. 22, pp. 119-133, January 01, 2013 2013.
- [9] H. Zhang, W. He, L. Zhang, H. Shen, and Q. Yuan, "Hyperspectral Image Restoration Using Low-Rank Matrix Recovery," IEEE Transactions on Geoscience and Remote Sensing, vol. 52, pp. 4729-4743, August 01, 2014 2014.
- [10] Y. Chen, X. Cao, Q. Zhao, D. Meng, and Z. Xu, "Denoising Hyperspectral Image With Non-i.i.d. Noise Structure," IEEE Transactions on Cybernetics, pp. 1-13.